High-definition tDCS to the right temporoparietal junction modulates slow-wave resting state power and coherence in healthy adults

Peter H. Donaldson[a]*, Melissa Kirkovski[a], Joel S. Yang[a], Soukayna Bekkali[a], Peter G. Enticott[a]

[a]*School of Psychology, Deakin University, Locked Bag 20000, Geelong, Victoria 3220, Australia*

*Corresponding author: Tel.: +613 9244 5504; fax: +613 924 46019; *email:* peter.donaldson@deakin.edu.au

Abstract

The right temporoparietal junction (rTPJ) is a multisensory integration hub that is increasingly utilised as a target of stimulation studies exploring its rich functional network roles and potential clinical applications. Whilst transcranial direct current stimulation (tDCS) is frequently employed in such studies, there is still relatively little known regarding its local and network neurophysiological effects, particularly at important non-motor sites such as the rTPJ. The current study applied either anodal, cathodal, or sham high-definition tDCS (HD-tDCS) to the rTPJ of 53 healthy participants and used offline electroencephalography (EEG) to assess the impacts of stimulation on resting state (eyes open and eyes closed) band power and coherence. Temporoparietal and central region delta power was increased after anodal stimulation (the latter trend only), whereas cathodal stimulation increased frontal region delta and theta power. Increased coherence between right and left temporoparietal regions was also observed after anodal stimulation. All significant effects occurred in the eyes open condition. These findings are discussed with reference to domain general and mechanistic theories of rTPJ function. Low frequency oscillatory activity may exert long-range inhibitory network influences that enable switching between and integration of endogenous/exogenous processing streams.

New & Noteworthy

Through the novel use of HD-tDCS and EEG, we provide evidence that both anodal and cathodal stimulation of the rTPJ selectively modulate slow-wave power and coherence in distributed network regions of known relevance to proposed TPJ functionality. These results also provide direct evidence of the ability of tDCS to modulate oscillatory activity at a long-range network level, which may have explanatory power in terms of both neurophysiological and behavioral effects.

high-definition transcranial direct current stimulation, electroencephalogram, temporoparietal junction, resting state, coherence

1. Introduction

Transcranial direct current stimulation (tDCS) is used broadly in neuroscience research due to its proposed neuromodulatory effects. However, the importance of better understanding the local and distributed neurophysiological effects of stimulation, particularly with regard to non-motor stimulation sites, has been increasingly recognised (Sellaro, Nitsche, & Colzato, 2016). There are many reasons that this understanding is important. First, assumptions are made regarding the likely effects and mechanisms of stimulation based on motor cortex research, which may not generalise to non-motor areas. Second, conclusions or claims are often made regarding the behavioural effects, or clinical relevance of, stimulating a particular region, without considering either distributed stimulation effects, or the stimulation montage employed. Finally, it is ultimately through an increased understanding of the underlying mechanisms of the effect of stimulation that the broad potential of technologies such as tDCS may be more fully realised.

The right temporoparietal junction (rTPJ) is a multisensory integration hub implicated in functional networks including attention/salience, memory, social cognition, and default mode networks (Carter & Huettel, 2013; Igelstrom, Webb, & Graziano, 2015; Igelström, Webb, Kelly, & Graziano, 2016; Kubit & Jack, 2013; R. Mars et al., 2012). While a number of domain-specific theories mapping onto involvement in these networks are posited, several domain-general theories regarding rTPJ processing/functionality also exist. These include the opposing domains and attentional breaking/reorienting hypotheses (Kubit & Jack, 2013), acting as an intero-exteroception ‘switch’ subserving integrative predictive processes (Bzdok et al., 2013), contextual updating of internal models (Geng & Vossel, 2013), and the nexus

model of Carter and Huettel (2013). The nexus model reasons that the TPJ is involved in multisensory and multinetwork integration processes that facilitate decision making, performance of complex tasks, and the establishment of a social context (Carter & Huettel, 2013). While these theories differ in nuance, they have in common the theme of a multinetwork integrative role for the TPJ in higher order processes. Such a role implies a need for strong communicative links, implying in turn a need for a mechanism for both local and distant communication, of which resting state network connectivity is one candidate mechanism. Studies examining rTPJ connectivity tend to advocate a parcellation approach and suggest that rTPJ sub-regions display varying levels of resting state and functional connectivity. Regions implicated comprise the aforementioned functional networks, particularly left temporoparietal sites and central/prefrontal structures (Bzdok et al., 2013; Carter & Huettel, 2013; Igelström et al., 2016; R. Mars et al., 2012). The rTPJ is also a site of increasing interest with reference to neuromodulatory studies and potential clinical relevance (Donaldson, Rinehart, & Enticott, 2015; Eddy, 2016).

Two ways of evaluating the electrophysiological network effects of rTPJ HD-tDCS are electroencephalographic (EEG) resting state power and coherence. Of relevance here is the principle that synchronous oscillations of neural assemblies at particular frequencies, even in non-proximal brain nodes/regions, may subserve brain network communication and function. Two related theories are the communication through coherence (CTC) hypothesis, and the gating by inhibition (GBI) hypothesis. The former (CTC) posits that neuronal communication is essentially facilitated by neuronal temporal synchronisation, with increased synchrony associated with increased functional communication/connectivity (Fries, 2005, 2015; Womelsdorf et al., 2007). The latter (GBI) essentially proposes that information routing between task-relevant regions is mediated by inhibiting/blocking activity in regions less relevant to the task (or current processing) (Jensen & Mazaheri, 2010). Importantly, both

theories may contribute to overall processing via low frequency/high frequency coupling, whereby higher frequency synchronous oscillations may be more associated with local task-related processing (and the CTC framework), and lower frequency oscillations may be critical to longer-range communication co-ordination (via the GBI framework) (Bonnefond, Kastner, & Jensen, 2017; Florin & Baillet, 2015).

Application of transcranial electrical stimulation (including tDCS) can influence neural oscillations and cognitive function, perhaps via direct and indirect influences on pyramidal cells and interneurons involved in glutamatergic and GABAergic transmission and local and distributed excitation/inhibition balances (Buzsáki, Anastassiou, & Koch, 2012; Harmony, 2013; Krause, Marquez-Ruiz, & Kadosh, 2013). This relates to the notion that the increased excitability frequently attributed to anodal tDCS is mediated by the effects of reduced local GABA and/or increased glutamate concentrations, which may have both local and network effects, a notion that has some support in motor cortex work (Stagg et al., 2014).

Annarumma, D'Atri, Alfonsi, and De Gennaro (2018) recently summarised results pertaining to both proximal and distal bandwidth power influences of tDCS, suggesting that anodal stimulation was associated with reduced slower wave power (delta, theta, alpha) but increased beta power, while cathodal stimulation increases slower wave power (delta, theta) and reduces beta and gamma power. Regarding the rTPJ more specifically, Spitoni, Di Russo, Cimmino, Bozzacchi, and Pizzamiglio (2013) applied anodal/cathodal/sham tDCS to the right posterior parietal cortex (rPPC: P2, P4, P6; noncephalic reference electrode), reporting that the only significant modulation was post-anodal stimulation increases in EEG parietal alpha power, and to a lesser extent, frontal alpha power. Mangia, Pirini, and Cappello (2014) applied the same protocol to the rPPC (P4; without a cathodal condition). Consistent with the findings of Spitoni et al. (2018), they reported significant increases in alpha power in parietal and frontal regions after anodal stimulation. Additionally, they observed increased theta

power parietocentrally during stimulation and frontally after stimulation, and increased beta power in parallel with the aforementioned alpha power modulation, though largely in contralateral parietal electrode sites. Based on these findings, Hsu, Tseng, Liang, Cheng, and Juan (2014) attempted to increase alpha power via rPPC (P4) anodal tDCS in a sample in order to examine subsequent effects on a visual memory task, but found alpha power *decreased* in the low-performing group and *did not change* in the high-performing group, which they interpreted through a lens of state-dependent tDCS effects. No studies could be identified examining the effects of TPJ tDCS on EEG coherence.

While these studies provide some evidence of stimulation influences on these important metrics of network dynamics, this short literature review also highlights the dearth of knowledge in this domain, further emphasising the need for increased understanding in such an important non-motor site as the rTPJ. These studies also used traditional tDCS, which is a disadvantage in terms of degree of acuity (due to large stimulation areas) when assessing and extrapolating with regard to local and distributed electrophysiological effects and potential impacts on function. This study sought to redress these limitations by using electroencephalography (EEG) to assess the impacts of anodal and cathodal rTPJ high-definition transcranial direct current stimulation (HD-tDCS) on resting state power and coherence with regards to key functional network regions associated with the rTPJ (frontal, central, and left TPJ electrode configurations). The limited number of directly relevant prior findings preclude confident directional hypotheses. However, based on the most directly relevant (PPC) studies discussed above, it was hypothesised that anodal stimulation (compared to cathodal and sham stimulation) would increase resting state power in theta, alpha, and beta bandwidths in the region of stimulation and functionally connected regions. It was also predicted that both active stimulation conditions would be associated with coherence changes in these regions compared to sham stimulation.

2. Materials and Methods

The present paper presents data collected as part of a larger study. The methodology therefore overlaps with that described previously in papers examining different aspects of the dataset (Donaldson, Kirkovski, Rinehart, & Enticott, 2018, 2019).

2.1. Participants

The sample comprised 53 right-handed healthy volunteers aged 18-40, with normal or corrected-to-normal vision and no contraindications to standard noninvasive brain stimulation screening protocols (Rossi, Hallett, Rossini, & Pascual-Leone, 2009) or history of mental illness, as determined by the MINI International Neuropsychological Interview Screen (Lecrubier et al., 1997). Participant demographics are outlined in Table 1. There were no significant differences between groups on any factor, with the exception of sex. The female to male ratio in sham, cathodal and anodal conditions were 10:8, 14:4, and 6:11, respectively (Cramer's $V = .35$, $p = .04$). Post-hoc testing indicated that cathodal and anodal conditions differed with regards to sex ($p = .03$). Time of day tested was also recorded and assessed, as it has been suggested that circadian factors and the physiology of sleep/wake states may mediate plasticity and responses to stimulation (Li, Uehara, & Hanakawa, 2015). Time of day tested did not differ between groups.

2.2. Design

The study was double-blind and sham-controlled with both within-subjects (pre- vs. post-stimulation) and between-subjects (stimulation condition; sham vs. cathodal vs. anodal stimulation) factors. Participants took part in one session, in which resting state EEG was recorded before and after 20 minutes of either sham, cathodal, or anodal HD-tDCS to the rTPJ. Protocols were approved by the human research ethics committee of Deakin University.

193 *2.3. Questionnaires*

194 Participants completed the Edinburgh Handedness Inventory (Oldfield, 1971) to
195 confirm right-handedness prior to participation. At the end of the session (after stimulation
196 and second EEG recording), participants completed a post-stimulation questionnaire.

197 *2.4. Procedure*

198 Participants were fitted with an EEG cap (www.easycap.de/), and the 10-20 system sites for
199 HD-tDCS electrodes were marked (Figures 1 and 2). The cap was then removed. HD-tDCS
200 electrode sites were cleaned with abrasive paste and alcohol swabs, before fixing five
201 electrodes (20mm diameter circular rubber, supplied by neuroConn;
202 www.neurocaregroup.com) into position with adhesive conductive paste. An impedance
203 check was carried out to ensure impedance was < 50 kΩ (neuroConn, 2014) prior to replacing
204 the EEG cap. HD-tDCS electrode positions were re-checked. Thirteen single silver-silver
205 chloride (Ag-AgCl) sintered ring EEG electrodes were fastened to the cap at the sites
206 displayed in Figure 1. EEG electrodes were also placed on each mastoid, above and below
207 the left eye, and on the lateral canthus of each eye. The ground electrode was placed centrally
208 on the forehead. Conductive gel was then applied to all EEG electrodes. Impedances were
209 kept below 5 kΩ where possible (with all impedances kept below 10 kΩ). Two experimenters
210 completed this setup process. The second experimenter then left the room before the next
211 stage.

212 Participants were seated in a darkened room, 60cm from the computer monitor
213 (www.benq.us/product/monitor/XL2420TE/specifications) at eye level. They sat for two
214 minutes during resting state (eyes open) EEG recording, during which they were instructed to
215 focus on a white fixation cross (15mm x 15mm) in the centre of the blackened screen
216 (280mm x 515mm). EEG was then recorded for two minutes while participants were asked to

keep their eyes closed.

At this point, the second experimenter returned to the room. The first experimenter then left the room to maintain blinding. An impedance check was again carried out on HD-tDCS electrodes. HD-tDCS was then applied to the rTPJ for 20 minutes (sham, cathodal, or anodal).

After HD-tDCS experimenter two left the room again and experimenter one returned. Participants again sat for two minutes during resting state (eyes open) EEG recording, followed by a further two minutes while participants were asked to keep their eyes closed. Finally, participants completed the post-stimulation questionnaire. *2.5. HD-tDCS*

The montage was chosen according to optimal current intensity and focality, based on Soterix neurotargeting software (http://soterixmedical.com/software). The configuration, current at each electrode, and modelling of stimulation intensity (for cathodal stimulation) are displayed in Figure 2. Stimulation was applied using a NeuroConn DC-Stimulator (MC Version; www.neurocaregroup.com). Active stimulation (anodal or cathodal) applied a current intensity of 2 mA (split evenly between electrodes) for 20 minutes, with a 30 second ramp-up and ramp-down at the beginning and end. Sham stimulation was also 20 minutes, but contained only three short, intermittent bursts of active 2 mA stimulation (totalling 230 seconds, each burst with a 30 second ramp-up and ramp-down). Participants were seated in a non-darkened room during stimulation, and were not engaged in any activities. EEG was not recorded during stimulation.

2.6. EEG recording and pre-processing

A 64-channel SynAmpsRT amplifier was used for acquisition (Compumedics Neuroscan, Charlotte, NC; http://compumedicsneuroscan.com). EEG recordings were in DC at a sampling rate of 1000 Hz.

EEG data were processed and analysed offline using Curry 7 Neuroimaging Suite (http://compumedicsneuroscan.com). Data were baseline corrected (constant), re-referenced to the average of the two mastoids, and band pass filtered (1-30 Hz). Oculomotor artefacts were identified (vertical, 100 uV; horizontal, 130 uV) and covaried. Bad blocks were also identified (±75 uV, as well as visually) and marked for exclusion from further analysis.

For resting state power analysis, back-to-back one-second epochs were saved and averaged. Power analysis was carried out across delta (1-3 Hz), theta (>3-8 Hz), alpha (>8-12 Hz) and beta (>12-30 Hz) bandwidths for each electrode. This was done using Fast Fourier Transformation (FFT) phase (time) option with a Hanning taper. This approach averages raw waveforms initially (time domain averaging), and subsequently computes FFT, which thereby takes phase relationships into account. Overall, 88% of epochs were retained for analysis for both eyes closed and open data sets. Electrodes were grouped and averaged for the left TPJ (lTPJ; CP5, P3, P7), rTPJ (CP6, P4, P8), central (C3, CZ, C4) and frontal (F3, FZ, F4) regions for further analysis.

Regarding coherence analysis, back-to-back three-second epochs were saved and averaged from each two-minute resting state data file. Complex demodulation was used in place of FFT in Curry for this purpose (Compumedics, 2011). A minimum of 10% acceptable epochs were required to be processed further. Minimum and maximum lag criteria for coherence values obtained were set at 2 ms and 10 ms, respectively. Electrodes were grouped into the same clusters as above - frontal (F3, FZ, F4), central (C3, CZ, C4), lTPJ (CP5, P7, P3) and rTPJ (CP6, P4, P8) - for averaging of individual electrode pairings and further analysis as per below.

2.7. Data analysis

All final statistical analyses were carried out in SPSS v. 22, IBM. Data were screened for normality and outliers. The latter were winsorised, and the appropriate procedures were adopted to manage the former (if distributions were non-normal, transformations were conducted in order to reduce skew/kurtosis according to Tabachnick and Fidell (2013)). Post-hoc tests with Bonferroni adjustments were used where appropriate. In contexts such as the present where multiple comparisons are conducted, control of family-wise error is a concern. Bootstrapping, a resampling method increasingly used in such contexts, selects and examines subsamples of a test population over numerous iterations (generally ≥ 1000 subsamples are preferred) in order to provide more information and make inferences regarding overall sample parameters. Bootstrapping provides more robust, accurate, and conservative estimates of p values and confidence intervals. It also assists with the reduction of Type I error risk, without compromising power (and therefore increasing Type II error) (Romano, Shaikh, & Wolf, 2010; Westfall & Troendle, 2008; Wright, London, & Field, 2011). Reviews of bootstrapping and its many applications are also available (Davison & Hinkley, 1997; Efron & Tibshirani, 1994). Bootstrapping was utilised in the case of significant findings to ensure these were robust (1000 samples, bias corrected accelerated). Details on bootstrapping and procedures in SPSS v. 22 are available at https://doi.org/10.6084/m9.figshare.9275909.

Other relevant materials also available on figshare include supplementary tables/figures (https://doi.org/10.6084/m9.figshare.8202107) and SPSS data files for resting state eyes closed (https://doi.org/10.6084/m9.figshare.8202137) and eyes open conditions (https://doi.org/10.6084/m9.figshare.8202134), as well as for coherence analysis (https://doi.org/10.6084/m9.figshare.8202116).

3. Results

3.1. Post-stimulation Questionnaire

Participants appeared to be well blinded to sham (only 39% correctly guessing), whereas 63% correctly identified an active condition. However, a chi-square test comparing correct responses versus incorrect/unsure responses was not significant ($p = .07$). All participants successfully completed stimulation. Two participants temporarily ceased due to discomfort, but completed stimulation after a short break (1-3 mins). A graphical summary of stimulation blinding and a table detailing stimulation-related experience/sensations are available on figshare at https://doi.org/10.6084/m9.figshare.8869208.

3.2. Resting state power analysis

3.2.1. Eyes Closed

Separate ANOVAs were used for frontal, central, and temporoparietal clusters, with log transformed power (uV^2) data. To examine possible hemispheric effects regarding the left and right TPJ clusters, a mixed model ANOVA with factors of time (pre, post), hemisphere (lTPJ, rTPJ), and condition (sham, cathodal, anodal) examined the impacts of stimulation on spectral power at each bandwidth. Results were non-significant for lower frequencies (delta, theta, and alpha; see Supplementary Table 1). A significant time x hemisphere x condition interaction was found at the beta bandwidth ($F(2, 50) = 3.69$, $p = .032$, $\eta_p^2 = .13$; Supplementary Table 2, Supplementary Figure 1). Post-hoc analyses, however, were not significant. Mixed model ANOVAs (with factors of time and condition only) were also conducted separately for frontal and central clusters. Results were not significant (Supplementary Tables 3 and 4).

3.2.2. Eyes Open

The same analyses were conducted for eyes open resting state data (also log transformed). Results were not significant for higher frequencies (Supplementary Tables 5-7).

There was no significant time x hemisphere x condition interaction for rTPJ versus lTPJ at any bandwidth. However, time x condition interactions were found in the delta bandwith for the TPJ ($F(2, 49) = 5.08$, $p = .010$, $\eta_p^2 = .17$) and central clusters ($F(2, 49) = 3.51$, $p = .037$, $\eta_p^2 = .13$), and in the theta bandwidth for the frontal cluster ($F(2, 49) = 4.27$, $p = .019$, $\eta_p^2 = .15$). A trend time x condition interaction was also found in the delta bandwith for the frontal cluster ($F(2, 49) = 3.19$, $p = .050$, $\eta_p^2 = .12$). Post-hoc analyses suggested that delta power was increased after anodal stimulation in both the TPJ ($t(15) = -2.71$, $p = .016$, $\eta^2 = .33$, Figure 3; $p = .019$ after bootstrapping) and central clusters ($t(15) = -2.22$, $p = .042$, $\eta^2 = .25$, Figure 4; $p = .052$ after bootstrapping), though the latter does not withstand Bonferroni correction at the revised alpha level of .0167 (and inflates to $p > .05$ with bootstrapping) and can be considered trend only (see also box and whisker representations of Figure 3 and Figure 4 at https://doi.org/10.6084/m9.figshare.8947439 and https://doi.org/10.6084/m9.figshare.8947445, respectively. The former must be interpreted with caution also given that the p value is marginally greater than .0167 also after bootstrapping. In frontal regions, power was increased after cathodal stimulation in both the theta bandwidth ($t(17) = -3.44$, $p = .003$, $\eta^2 = .44$, Figure 5; $p = .002$ after bootstrapping) and delta bandwidth ($t(17) = -3.04$, $p = .007$, $\eta^2 = .38$, Figure 6; $p = .003$ after bootstrapping). Please note that these figures display log transformed means (see also box and whiskers representations at https://doi.org/10.6084/m9.figshare.8947448 and https://doi.org/10.6084/m9.figshare.8947454, respectively). Several main effects of time were also observed (Supplementary Tables 5-10).

3.3. Coherence analysis

Coherence value difference scores (pre-stimulation subtracted from post-stimulation) were used due to improved distribution normality compared to pre- and post-distributions,

meaning that data transformations were not necessary for coherence analyses. Difference scores were calculated for each pre-identified electrode pairing for each participant at each bandwidth, averaged across epochs (e.g. F3-CP6, F3-P4, F3-P8). These were then averaged across each region cluster pairing: rTPJ-frontal (CP6, P4, P8 - F3, FZ, F4), rTPJ-central (CP6, P4, P8 - C3, CZ, C4), rTPJ-lTPJ (CP6, P4, P8 – CP5, P7, P3). Only coherence pairs that begin and terminate in different regions were used for the averaged data.

3.3.1. Eyes Closed

An average of 87% of cases were retained for analyses (Supplementary Table 11). One-way ANOVAs examined coherence difference scores (post-pre) in each cluster pairing at each bandwidth, with stimulation condition as the factor. Results were non-significant in all cases (Supplementary Table 12).

3.3.2. Eyes Open

The same analyses were conducted for eyes open data. An average of 93% of cases were retained for analyses (Supplementary Table 13). Although rTPJ-central region pairings neared significance in the theta band (see Supplementary Table 14 for full summary statistics), the only statistically significant difference observed was in the rTPJ-lTPJ pairing in the delta band, $F(2, 49) = 3.90$, $p = .027$, $\eta_p^2 = .14$. Post-hoc analyses suggested that rTPJ-lTPJ delta power coherence was increased after anodal stimulation compared to cathodal stimulation ($t(32) = 2.70$, $p = .011$ (p = .012 after bootstrapping), $\eta^2 = .19$) and sham stimulation ($t(32) = 2.10$, $p = .043$ (p = .041 after bootstrapping), $\eta^2 = .12$), though the latter does not withstand Bonferroni correction at the revised alpha level of .0167 and can be considered trend only. Figure 7 displays this result graphically (see also box and whiskers representation at https://doi.org/10.6084/m9.figshare.8947457). Positive mean differences indicate increased coherence between regions after stimulation, and therefore increased rTPJ-

lTPJ coherence after anodal stimulation in the delta bandwidth (compared to cathodal, and trending compared to sham).

4. Discussion

This study applied anodal, cathodal, or sham HD-tDCS to the rTPJ in order to examine local and distributed modulatory effects at a neurophysiological level, via resting state EEG power and coherence. To our knowledge it is the first study to do so. Results of the present study can be both compared and contrasted with prior findings that informed the present hypotheses (which were only partially supported), and will be discussed according to the following themes: (1) active HD-tDCS modulated both local and network resting state power, but this occurred at low frequencies (particularly in the delta bandwidth), and not in the alpha/beta bandwidths as previously reported; (2) anodal HD-tDCS increased lTPJ-rTPJ interhemispheric coherence in the delta bandwidth only; (3) modulatory effects were almost exclusively observed in the eyes open (EO) rather than eyes closed (EC) condition, directly contrasting with prior groups findings.

1. Delta/theta power modulated by active HD-tDCS

In contrast to prior findings (Mangia et al., 2014; Spitoni et al., 2013), active stimulation did not increase resting state power in alpha or beta bandwidths. This null finding, however, is consistent with Hsu et al. (2014), who used the same tDCS protocol (targeting P4) as the other groups in attempting to increase alpha power, but found no alpha modulation after anodal stimulation in what were categorised as high-performers on a subsequent visual memory task, and *reduced* alpha power in low-performers. The authors interpreted this as a-priori state/trait based network oscillatory differences leading to differences in susceptibility/modulability by tDCS. Such individual differences may have contributed to variation in the present sample that reduced the power to detect higher

384 frequency modulatory effects. Another difference between the present and prior studies is the
385 use of HD-tDCS, which uses much smaller electrodes with greater current densities to elicit
386 more localised stimulation effects. Such differences may also lead to different local and
387 network neural/neurotransmitter impacts that result in different oscillatory profile effects.
388 The consistent finding of increases in delta power across frontal regions after cathodal
389 stimulation, and central/temporoparietal regions after anodal stimulation (in some instances
390 trend only) was interesting and somewhat unexpected. That cathodal stimulation specifically
391 modulated distal frontal regions in contrast to the more proximal regions modulated by
392 anodal stimulation raises questions regarding differing oscillatory influences and mechanisms
393 of action of the two current polarities, though the present methodology cannot shed further
394 light on this potential distinction. More broadly, delta power increases after cathodal motor
395 cortex tDCS have been previously observed (Ardolino, Bossi, Barbieri, & Priori, 2005), and
396 are consistent with the anodal-excitation/cathodal-inhibition (Ae/Ci) hypothesis of tDCS
397 neuronal excitability effects: if cathodal stimulation inhibits, increased slow-wave power
398 might be expected. Increased delta power after anodal stimulation contrasts with many prior
399 studies (Annarumma et al., 2018; Keeser et al., 2011; Wirth et al., 2011), though these
400 involve frontal rather than temporoparietal stimulation. Consistent with current findings,
401 however, Boonstra, Nikolin, Meisener, Martin, and Loo (2016) observed anodal stimulation
402 *increases* in resting state delta power after frontal tDCS. These authors highlighted the
403 relevance of EO versus EC resting state conditions, a point which will be pursued further
404 below. They also interpreted this deviation from prior findings from the perspective of
405 differing electrode size and current densities, noting that increased charge densities and
406 therefore stimulation intensities can alter and even reverse normal Ae/Ci effects in the motor
407 cortex. In one such study, 20 minutes of 2 mA cathodal tDCS (as applied here) produced
408 increased cortical excitability rather than inhibition (Batsikadze, Moliadze, Paulus, Kuo, &

409 Nitsche, 2013). In general, the present study also adds support to the notion that the
410 traditional Ae/Ci model of tDCS effects is problematic, particularly in non-motor regions,
411 and may also be state-dependant and influenced by intra- and inter-individual differences not
412 controlled or accounted for in studies such as the present one (Horvath, Carter, & Forte,
413 2014; Krause & Kadosh, 2014).

414 The finding that delta/theta power in frontal regions increased after cathodal
415 stimulation is, however, consistent with the traditional Ae/Ci perspective. While this has been
416 observed previously at a local level in the motor cortex (Ardolino et al., 2005), this was not
417 reported after rPPC cathodal stimulation in another study (Spitoni et al., 2013). Mangia et al.
418 (2014), however, did find an increase in theta power during *anodal* rPPC stimulation that
419 began locally and propagated forward to frontocentral regions after stimulation, and
420 particularly frontal regions in the EO condition. As above, methodological differences
421 between studies, such as varying charge densities, may at least partly explain inconsistent
422 findings. The potential meaning and implication of these findings will be discussed after
423 some brief statements on the coherence findings, as these are also relevant to the
424 interpretation.

425 ***2. Anodal HD-tDCS increased lTPJ-rTPJ coherence in the delta bandwidth only***

426 Consistent with the themes above, interhemispheric TPJ delta coherence was
427 increased after anodal stimulation. Combined with the increases in distributed resting state
428 delta power post stimulation noted above, these findings raise questions regarding both the
429 importance of slow wave activity to distal communication/connectivity, and the potential
430 functional implications of such modulations, given the proposed roles of the rTPJ. While
431 slow frequency resting state oscillations have traditionally been associated with drowsy and
432 sleep states (Annarumma et al., 2018), it is unlikely that the present results can be interpreted

433 through a lens of increased drowsiness as the study session progressed. If this were the case,
434 increased slow wave power and coherence might be expected after sham compared to active
435 stimulation, and in the eyes closed rather than eyes open condition, the reverse of the pattern
436 observed here.

437 Informing alternative interpretations, it is increasingly recognised that delta
438 oscillatory activity may have other functional significance in both the resting and task-
439 oriented brain (Harmony, 2013). In a detailed review, Knyazev (2012) posits a critical role
440 for delta oscillations in terms of synchronising cortical and autonomic functions, listing
441 motivation/reward and attention/salience processes as strongly implicated. In another
442 informative review, Harmony (2013) proposes a model that bridges the task-oriented/resting
443 brain and sleep literature, by suggesting that delta oscillations may down-modulate the
444 activity of brain networks not supporting current processing/mentation (for example, to
445 inhibit sensory afferences and facilitate internally directed attention/concentration). This
446 aligns with the GBI framework discussed in the introduction (Jensen & Mazaheri, 2010).
447 Combined with the principle that large networks tend to be recruited during slow wave
448 oscillations (as opposed to higher frequencies association with more local networks) (Lu et
449 al., 2007; Silberstein, 2006; von Stein & Sarnthein, 2000), it is plausible to hypothesise in the
450 context of present results, that slow wave oscillatory activity might be one means by which
451 the rTPJ might contribute to its proposed integrative effects and functions across domains and
452 networks, including a role in mediating between endogenous/exogenous attention and
453 processing, and influencing the activity of relevant and irrelevant networks. Frontoparietal
454 and interhemispheric lTPJ-rTPJ structural and functional connectivity may be particularly
455 important in this regard.

456 ***3. Modulatory effects were almost exclusively observed in the eyes open (EO) rather than***
457 ***eyes closed (EC) condition***

458 Prior papers, including two rPPC tDCS studies (Mangia et al., 2014; Spitoni et al.,
459 2013), tend to find greater oscillatory responsiveness to tDCS in the EC rather than EO
460 condition. More general research into differences between EO and EC conditions in EEG
461 suggest a general reduction in delta, theta, and alpha power in EO compared to EC, taken to
462 reflect the processing of visual stimuli necessitating higher frequency oscillations in relevant
463 networks (Barry, Clarke, Johnstone, & Brown, 2009; Barry, Clarke, Johnstone, Magee, &
464 Rushby, 2007). More specifically, Mangia et al. (2014, p. 6) apply this to their interpretation
465 by suggesting that the brain may have a greater sensitivity to tDCS in the EC condition as "a
466 consequence of a higher processing capability to the external tDCS stimuli available."
467 While it is possible our differing result is the consequence of methodological
468 differences or statistical anomaly, alternative interpretations are available in line with the
469 rTPJ functional connectivity discussed in the prior section. More specifically, it is well
470 established that the brain is not 'resting' during so called resting states, despite the absence of
471 exogenous visual input in EC conditions. Of relevance here is the proposed default mode
472 network (DMN), a network of structures including the bilateral TPJ and medial frontal
473 regions that tend to be more active 'at rest' (or during endogenous attention processes such as
474 autobiographical memory retrieval, considering the perspectives of others, and imagining
475 future situations) and anticorrelated with exogenous or task-focused attention networks
476 (Buckner, Andrews-Hanna, & Schacter, 2008; Greicius, Krasnow, Reiss, & Menon, 2003; R.
477 Mars et al., 2012). It is unlikely that in EO conditions - such as the current one - where
478 participants are asked to gaze at a fixation cross on a screen for several minutes, that they can
479 or do consciously attend to the cross for that duration. It is more likely that after a brief
480 period, participants continue to gaze at the cross as their mind 'wanders' in the manner
481 described above, implicating DMN activity and associated anticorrelated deactivations.
482 Consistent with this, Yan et al. (2009) examined functional connectivity and regional

amplitude of low frequency fluctuation (ALFF) in DMN regions in three resting state fMRI conditions: EC, EO (with fixation; EO-F), EO (without fixation; EO-WF). They reported greater functional connectivity and ALFF in DMN regions in both EO conditions compared to EC, and greater functional connectivity in many regions (as well as ALFF in some regions) in EO-F compared to EO-WF. Yan et al. (2009, p. 9) take this to reflect more highly synchronised and greater spontaneous neuronal activity in DMN regions in EO compared to EC conditions, and suggest that EO conditions may be associated with "more nonspecific or non-goal-directed visual information gathering and evaluating, as well as mind wandering and daydreaming." While speculative, linking this with the present discussion and results, one interpretation might be that in EO conditions, increased DMN activity associated with activities such as episodic memory processing or mind wandering might require more down-regulation of sensory afferences (and their salience attributions), particularly exogenous visual stimuli processing, and that broad low frequency oscillatory network activity may be one means by which this is achieved. Furthermore, if this is more 'effortful' in active conditions, this might partly explain why active rTPJ stimulation conditions exerted low frequency network oscillatory activity influences in EO conditions only. Contrasting again with a prior rPPC tDCS study, Spitoni et al. (2013) verbally requested participants open or close eyes every 30 seconds for 15 minutes, which would have different network dynamic effects to the protocol used here (2 minutes of EO, 2 minutes of EC), and would mean the initial network effects/response to opening one's eyes (i.e. the effects of the visual input and the period of the system inhibiting these afferences if wishing to return to DMN processing) would make up a greater percentage of epochs used for resting state analysis, and likely produce very different results.

Limitations

One important methodological limitation is the partial EEG montage. While this was partly necessary given the physical interference of HD-tDCS electrodes, it does limit both spatial resolution and the capacity to assess more global effects. Adding to this, electrode potentials were grouped and averaged for a priori regions of interest for final analyses, further reducing spatial resolution. The use of mastoids as reference is also potentially a limitation in terms of EEG signal bias (Joyce & Rossion, 2005). However, this was partially offset by averaging the mastoids for analysis. A further limitation was the sex imbalance in the cathodal condition, which had a higher male to female ratio than the anodal condition. While sex may interact with resting state EEG measures, a recent review suggests that evidence for this is minimal and inconsistent in healthy samples, and that such analyses in prior studies were secondary in nature and had not systematically examined resting state sex differences (Sanders, 2017). An associated study directly testing resting state EEG sex differences found increased beta power (at three frontocentral electrode sites) as the only significant difference between sexes in in women compared to men (across a healthy group and a group with schizophrenia) (Sanders, 2017). Similarly, state-dependent influences of tDCS may include factors relevant to sex such as hormone levels (Krause & Kadosh, 2014). However, at present we are unaware of any evidence suggesting sex differences in resting state EEG outcomes related to tDCS effects in healthy samples, although the reverse – the absence of sex differences – has been reported (Accornero et al., 2014). It is therefore unlikely that sex would exert a significant influence in the present healthy and high-functioning (largely university sourced) sample, although results should be interpreted cautiously in this regard. An additional limitation is the lack of behavioural outcome measures linked to proposed rTPJ functions, which reduces the capacity for the findings and present discussion to link strongly and directly with TPJ function. Finally, it must also be acknowledged that the study was likely underpowered, which may at least partially account for several of the null findings that

counter present hypotheses or past results. Related to this is the possibility of type I error in the context of multiple comparisons without full Bonferroni adjustment. However, it is encouraging that all significant findings occurred only in slow-wave, eyes-open, active stimulation conditions, and that p values were robust to bootstrapping. Given the relative dearth of HD-tDCS-EEG oscillation reports in non-motor areas, we consider it important to report all analyses conducted and consider our statistical approach an appropriate compromise between risk of type I and type II error. Nonetheless, our results must be considered preliminary, be interpreted cautiously, and await further replication.

Conclusion

This study applied HD-tDCS to the rTPJ to examine neuromodulatory effects via resting state EEG power and coherence. Results suggested that modulations of oscillatory activity at low frequency bandwidths (particularly delta) were more likely to occur than at higher frequencies, and in eyes open compared to eyes closed conditions. Results were not uniformly consistent with the traditional Ae/Ci model of tDCS effects, adding support to the notion that this model applies less reliably to non-motor sites, or may become more complex in terms of dependence on state/trait/topography differences in non-motor regions. Although the present data set can only be considered preliminary, it does point to the need for further analysis of delta oscillatory activity with respect to rTPJ function and connectivity. Future studies would benefit from larger sample sizes to examine subtle neuromodulatory effects and could also consider study designs that might inform a broader discussion. This might include the utilisation of behavioural outcomes relevant to the different implicit rTPJ functional networks, and additional methodologies such as magnetic resonance spectroscopy that might assist with assessing tDCS effects on underlying neurotransmitter concentrations, which may in turn map on to local and distributed network activity and behavioural

556 outcomes.

557
558 **Grants**

559 Peter Enticott is supported by a Future Fellowship from the Australian Research
560 Council (ARC) (FT160100077).

561 **Disclosures**

562 No competing financial interests are declared by the author. The contents of this paper
563 are original and have not been published.

564 **Author Contributions**

565 P.G.E. and P.H.D. conceived and designed research; P.H.D and M.K. performed
566 experiments; P.H.D. and J.S.Y. analysed data; P.G.E., P.H.D., M.K., J.S.Y and S.B.
567 interpreted results of experiments; P.H.D. and J.S.Y. prepared figures; P.H.D. drafted
568 manuscript; P.G.E., P.H.D., M.K., J.S.Y and S.B. edited and revised manuscript; P.G.E.,
569 P.H.D., M.K., J.S.Y and S.B. approved final version of manuscript. The authors would also
570 like to thank Charlotte Davies and Natalia Albein-Urios, who contributed to data collection,
571 and George Youssef, who provided statistical advice.

572
573
574
575
576
577
578

579 **References**

580 Accornero, N., Capozza, M., Pieroni, L., Pro, S., Davì, L., & Mecarelli, O. (2014). EEG
581 mean frequency changes in healthy subjects during prefrontal transcranial direct
582 current stimulation. *J. Neurophysiol., 112*(6), 1367-1375.
583 doi:10.1152/jn.00088.2014
584 Annarumma, L., D'Atri, A., Alfonsi, V., & De Gennaro, L. (2018). The efficacy of
585 transcranial current stimulation techniques to modulate resting-state EEG, to affect
586 vigilance and to promote sleepiness. *Brain Sci., 8*(7), 137.
587 doi:10.3390/brainsci8070137
588 Ardolino, G., Bossi, B., Barbieri, S., & Priori, A. (2005). Non-synaptic mechanisms
589 underlie the after-effects of cathodal transcutaneous direct current stimulation of
590 the human brain. *J. Physiol., 568*(2), 653-663. doi:10.1113/jphysiol.2005.088310
591 Barry, R. J., Clarke, A. R., Johnstone, S. J., & Brown, C. R. (2009). EEG differences in
592 children between eyes-closed and eyes-open resting conditions. *Clin.*
593 *Neurophysiol., 120*(10), 1806-1811. doi:10.1016/j.clinph.2009.08.006
594 Barry, R. J., Clarke, A. R., Johnstone, S. J., Magee, C. A., & Rushby, J. A. (2007). EEG
595 differences between eyes-closed and eyes-open resting conditions. *Clin.*
596 *Neurophysiol., 118*(12), 2765-2773. doi:10.1016/j.clinph.2007.07.028
597 Batsikadze, G., Moliadze, V., Paulus, W., Kuo, M. F., & Nitsche, M. A. (2013). Partially
598 non-linear stimulation intensity-dependent effects of direct current stimulation on
599 motor cortex excitability in humans. *J. Physiol., 591*(7), 1987-2000.
600 doi:10.1113/jphysiol.2012.249730
601 Bonnefond, M., Kastner, S., & Jensen, O. (2017). Communication between Brain Areas
602 Based on Nested Oscillations. *eNeuro, 4*(2), ENEURO.0153-0116.2017.
603 doi:10.1523/eneuro.0153-16.2017
604 Boonstra, T. W., Nikolin, S., Meisener, A.-C., Martin, D. M., & Loo, C. K. (2016). Change

in mean frequency of resting-state electroencephalography after transcranial direct current stimulation. *Front. Hum. Neurosci., 10*(270). doi:10.3389/fnhum.2016.00270

Buckner, R. L., Andrews-Hanna, J. R., & Schacter, D. L. (2008). The brain's default network: Anatomy, function, and relevance to disease. *Ann. N. Y. Acad. Sci, 1124*, 1-38. doi:10.1196/annals.1440.011

Buzsáki, G., Anastassiou, C. A., & Koch, C. (2012). The origin of extracellular fields and currents — EEG, ECoG, LFP and spikes. *Nat. Rev. Neurosci., 13*, 407. doi:10.1038/nrn3241

Bzdok, D., Langner, R., Schilbach, L., Jakobs, O., Roski, C., Caspers, S., . . . Eickhoff, S. B. (2013). Characterization of the temporo-parietal junction by combining data-driven parcellation, complementary connectivity analyses, and functional decoding. *NeuroImage, 81*, 381-392. doi:10.1016/j.neuroimage.2013.05.046

Carter, R. M., & Huettel, S. A. (2013). A nexus model of the temporal-parietal junction. *Trends Cogn. Sci., 17*(7), 328-336. doi:10.1016/j.tics.2013.05.007

Compumedics, N. (2011). *CURRY Neuroimaging Suite Installation and Tutorials: Multi-modal neuroimaging for CURRY 7*. United States of America: Compumedics USA, Inc.

Davison, A. C., & Hinkley, D. V. (1997). *Bootstrap methods and their application*: Cambridge University Press.

Donaldson, P. H., Kirkovski, M., Rinehart, N. J., & Enticott, P. G. (2018). Autism-relevant traits interact with temporoparietal junction stimulation effects on social cognition: a high-definition transcranial direct current stimulation and electroencephalography study. *Eur. J. Neurosci., 47*(6), 669-681. doi:10.1111/ejn.13675

Donaldson, P. H., Kirkovski, M., Rinehart, N. J., & Enticott, P. G. (2019). A double-blind HD-tDCS/EEG study examining right temporoparietal junction involvement in

facial emotion processing. *Soc. Neurosci.* doi:10.1080/17470919.2019.1572648

Donaldson, P. H., Rinehart, N. J., & Enticott, P. G. (2015). Noninvasive stimulation of the temporoparietal junction: A systematic review. *Neurosci. Biobehav. Rev., 55*(0), 547-572. doi:10.1016/j.neubiorev.2015.05.017

Eddy, C. M. (2016). The junction between self and other? Temporo-parietal dysfunction in neuropsychiatry. *Neuropsychologia*. doi:10.1016/j.neuropsychologia.2016.07.030

Efron, B., & Tibshirani, R. J. (1994). *An introduction to the bootstrap*: CRC press.

Florin, E., & Baillet, S. (2015). The brain's resting-state activity is shaped by synchronized cross-frequency coupling of neural oscillations. *NeuroImage, 111*, 26-35. doi:10.1016/j.neuroimage.2015.01.054

Fries, P. (2005). A mechanism for cognitive dynamics: Neuronal communication through neuronal coherence. *Trends Cogn. Sci., 9*(10), 474-480. doi:10.1016/j.tics.2005.08.011

Fries, P. (2015). Rhythms for cognition: Communication through coherence. *Neuron, 88*(1), 220-235. doi:10.1016/j.neuron.2015.09.034

Geng, J. J., & Vossel, S. (2013). Re-evaluating the role of TPJ in attentional control: Contextual updating? *Neurosci. Biobehav. Rev., 37*(10 Pt 2), 2608-2620. doi:10.1016/j.neubiorev.2013.08.010

Greicius, M. D., Krasnow, B., Reiss, A. L., & Menon, V. (2003). Functional connectivity in the resting brain: A network analysis of the default mode hypothesis. *Proc. Natl. Acad. Sci., 100*(1), 253-258. doi:10.1073/pnas.0135058100

Harmony, T. (2013). The functional significance of delta oscillations in cognitive processing. *Front. Integr. Neurosci., 7*, 83-83. doi:10.3389/fnint.2013.00083

Horvath, J., Carter, O., & Forte, J. D. (2014). Transcranial direct current stimulation: Five important issues we aren't discussing (but probably should be). *Front. Syst. Neurosci., 8*(2), 1-8. doi:10.3389/fnsys.2014.00002

657 Hsu, T.-Y., Tseng, P., Liang, W.-K., Cheng, S.-K., & Juan, C.-H. (2014). Transcranial
658 direct current stimulation over right posterior parietal cortex changes prestimulus
659 alpha oscillation in visual short-term memory task. *NeuroImage, 98*, 306-313.
660 doi:10.1016/j.neuroimage.2014.04.069
661 Igelstrom, K. M., Webb, T. W., & Graziano, M. S. (2015). Neural processes in the human
662 temporoparietal cortex separated by localized independent component analysis. *J.*
663 *Neurosci., 35*(25), 9432-9445. doi:10.1523/jneurosci.0551-15.2015
664 Igelström, K. M., Webb, T. W., Kelly, Y. T., & Graziano, M. S. A. (2016). Topographical
665 organization of attentional, social, and memory processes in the human
666 temporoparietal cortex. *eNeuro, 3*(2). doi:10.1523/ENEURO.0060-16.2016
667 Jensen, O., & Mazaheri, A. (2010). Shaping functional architecture by oscillatory alpha
668 activity: Gating by inhibition. *Front. Hum. Neurosci., 4*(186).
669 doi:10.3389/fnhum.2010.00186
670 Joyce, C., & Rossion, B. (2005). The face-sensitive N170 and VPP components manifest
671 the same brain processes: The effect of reference electrode site. *Clin.*
672 *Neurophysiol., 116*(11), 2613-2631. doi:10.1016/j.clinph.2005.07.005
673 Keeser, D., Padberg, F., Reisinger, E., Pogarell, O., Kirsch, V., Palm, U., . . . Mulert, C.
674 (2011). Prefrontal direct current stimulation modulates resting EEG and event-
675 related potentials in healthy subjects: a standardized low resolution tomography
676 (sLORETA) study. *NeuroImage, 55*(2), 644-657.
677 doi:10.1016/j.neuroimage.2010.12.004
678 Knyazev, G. G. (2012). EEG delta oscillations as a correlate of basic homeostatic and
679 motivational processes. *Neurosci. Biobehav. Rev., 36*(1), 677-695.
680 doi:10.1016/j.neubiorev.2011.10.002
681 Krause, B., & Kadosh, R. C. (2014). Not all brains are created equal: The relevance of
682 individual differences in responsiveness to transcranial electrical stimulation.

Front. Syst. Neurosci., 8, 25. doi:10.3389/fnsys.2014.00025

Krause, B., Marquez-Ruiz, J., & Kadosh, R. C. (2013). The effect of transcranial direct current stimulation: A role for cortical excitation/inhibition balance? *Front. Hum. Neurosci., 7*, 602. doi:10.3389/fnhum.2013.00602

Kubit, B., & Jack, A. I. (2013). Rethinking the role of the rTPJ in attention and social cognition in light of the opposing domains hypothesis: Findings from an ALE-based meta-analysis and resting-state functional connectivity. *Front. Hum. Neurosci., 7*, 323. doi:10.3389/fnhum.2013.00323

Lecrubier, Y., Sheehan, D. V., Weiller, E., Amorim, P., Bonora, I., Harnett Sheehan, K., . . . Dunbar, G. C. (1997). The Mini International Neuropsychiatric Interview (MINI). A short diagnostic structured interview: Reliability and validity according to the CIDI. *Eur. Psychiatry, 12*(5), 224-231. doi:10.1016/S0924-9338(97)83296-8

Li, L. M., Uehara, K., & Hanakawa, T. (2015). The contribution of interindividual factors to variability of response in transcranial direct current stimulation studies. *Front. Cell. Neurosci., 9*, 181. doi:10.3389/fncel.2015.00181

Lu, H., Zuo, Y., Gu, H., Waltz, J. A., Zhan, W., Scholl, C. A., . . . Stein, E. A. (2007). Synchronized delta oscillations correlate with the resting-state functional MRI signal. *Proc. Natl. Acad. Sci. U. S. A., 104*(46), 18265. doi:10.1073/pnas.0705791104

Mangia, A. L., Pirini, M., & Cappello, A. (2014). Transcranial direct current stimulation and power spectral parameters: a tDCS/EEG co-registration study. *Front. Hum. Neurosci., 8*(601). doi:10.3389/fnhum.2014.00601

Mars, R., Neubert, F.-X., Noonan, M., Sallet, J., Toni, I., & Rushworth, M. (2012). On the relationship between the “default mode network” and the “social brain”. *Front. Hum. Neurosci., 6*(189). doi:10.3389/fnhum.2012.00189

Mars, R., Sallet, J., Schüffelgen, U., Jbabdi, S., Toni, I., & Rushworth, M. F. S. (2012).

Connectivity-based subdivisions of the human right “temporoparietal junction area”: Evidence for different areas participating in different cortical networks. *Cerebral Cortex, 22*(8), 1894-1903. doi:10.1093/cercor/bhr268

neuroConn. (2014). neuroconn programmable direct current stimulator user's manual (MC version): neuroConn GmbH

Oldfield, R. C. (1971). The assessment and analysis of handedness: The Edinburgh Inventory. *Neuropsychologia, 9*(1), 97-113. doi:10.1016/0028-3932(71)90067-4

Romano, J. P., Shaikh, A. M., & Wolf, M. (2010). Multiple testing *The New Palgrave Dictionary of Economics* Palgrave Macmillan.

Rossi, S., Hallett, M., Rossini, P. M., & Pascual-Leone, A. (2009). Safety, ethical considerations, and application guidelines for the use of transcranial magnetic stimulation in clinical practice and research. *Clin. Neurophysiol., 120*(12), 2008-2039. doi:10.1016/j.clinph.2009.08.016

Sanders, K. M. (2017). *Demographic Differences in Resting State EEG in Healthy Controls and Patients with Schizophrenia.* Loma Linda University Electronic Theses, Dissertations & Projects. Retrieved from http://scholarsrepository.llu.edu/etd/488 (488)

Sellaro, R., Nitsche, M. A., & Colzato, L. S. (2016). The stimulated social brain: Effects of transcranial direct current stimulation on social cognition. *Ann. N. Y. Acad. Sci., 1369*(1), 218-239. doi:10.1111/nyas.13098

Silberstein, R. B. (2006). Dynamic sculpting of brain functional connectivity and mental rotation aptitude. In C. Neuper & W. Klimesch (Eds.), *Progress in brain research* (Vol. 159, pp. 63-76): Elsevier.

Spitoni, G., Di Russo, F., Cimmino, R. L., Bozzacchi, C., & Pizzamiglio, L. (2013). Modulation of spontaneous alpha brain rhythms using low-intensity transcranial direct-current stimulation. *Front. Hum. Neurosci., 7*(529).

doi:10.3389/fnhum.2013.00529

Stagg, C. J., Bachtiar, V., Amadi, U., Gudberg, C. A., Ilie, A. S., Sampaio-Baptista, C., . . . Johansen-Berg, H. (2014). Local GABA concentration is related to network-level resting functional connectivity. *eLife, 3*, e01465. doi:10.7554/eLife.01465

Tabachnick, B. G., & Fidell, L. S. (2013). *Using multivariate statistics* (Sixth ed.). Boston: Pearson Education

von Stein, A., & Sarnthein, J. (2000). Different frequencies for different scales of cortical integration: from local gamma to long range alpha/theta synchronization. *Int. J. Psychophysiol., 38*(3), 301-313.

Westfall, P. H., & Troendle, J. F. (2008). Multiple testing with minimal assumptions. *Biometrical journal. Biometrische Zeitschrift, 50*(5), 745-755. doi:10.1002/bimj.200710456

Wirth, M., Rahman, R. A., Kuenecke, J., Koenig, T., Horn, H., Sommer, W., & Dierks, T. (2011). Effects of transcranial direct current stimulation (tDCS) on behaviour and electrophysiology of language production. *Neuropsychologia, 49*(14), 3989-3998. doi:10.1016/j.neuropsychologia.2011.10.015

Womelsdorf, T., Schoffelen, J.-M., Oostenveld, R., Singer, W., Desimone, R., Engel, A. K., & Fries, P. (2007). Modulation of neuronal interactions through neuronal synchronization. *Science, 316*(5831), 1609. doi:10.1126/science.1139597

Wright, D. B., London, K., & Field, A. P. (2011). Using Bootstrap Estimation and the Plug-in Principle for Clinical Psychology Data. *Journal of Experimental Psychopathology, 2*(2), 252-270. doi:10.5127/jep.013611

Yan, C., Liu, D., He, Y., Zou, Q., Zhu, C., Zuo, X., . . . Zang, Y. (2009). Spontaneous brain activity in the default mode network is sensitive to different resting-state conditions with limited cognitive load. *PLoS ONE, 4*(5), e5743. doi:10.1371/journal.pone.0005743

761

762

Table 1

Demographic characteristics as per group.

Variable	Sham (n = 18)		Cathodal (n = 18)		Anodal (n =17)		ANOVA statistics	
	M	*SD*	*M*	*SD*	*M*	*SD*	*F*	*p*
Age	26.5	6.6	24.4	4.4	24.3	5.4	0.90	.41
Years of education	17	2.6	17.3	2.6	17.4	3.4	0.10	.91
Time of day tested	11:34	2.6	11:52	2.6	11:00	2.4	0.20	.82
EHI	0.88	0.2	0.83	0.2	0.85	0.2	0.24	.79

Note: EHI = Edinburgh Handedness Inventory

763

764 **Fig. 1**. Diagram of EEG electrode layout (green circles) and HD-tDCS electrode montage (yellow circles 0.5
765 mA each, navy blue circle 2 mA, polarity depending on anodal or cathodal condition). Electrodes were also
766 placed on each mastoid, above and below the left eye, and on the lateral canthus of each eye. The ground
767 electrode was placed centrally on the forehead.

768 **Fig. 2.** Montage and Soterix modelling for cathodal stimulation of the rTPJ. Polarities are reversed for anodal
769 stimulation. For anodal stimulation, the central electrode (P6) was the anode, with the other four electrodes
770 (C6, TP8, PO8, P2) collectively forming the cathode (see also Figure 1). The reverse polarity arrangement
771 constituted cathodal stimulation.
772
773 **Fig. 3.** Effect of condition (sham, cathodal, and anodal) on TPJ delta power (pooled across rTPJ and lTPJ,
774 log transformed uV^2) during resting state (eyes open). Note: Error bars represent SE; $p = .019$ after
775 bootstrapping in anodal condition.
776
777 **Fig. 4.** Effect of condition (sham, cathodal, and anodal) on delta power (pooled across central electrodes, log
778 transformed uV^2) during resting state (eyes open). Note: Error bars represent SE; $p = .052$ after bootstrapping
779 in anodal condition.
780
781 **Fig. 5.** Effect of condition (sham, cathodal, and anodal) on theta power (pooled across frontal electrodes, log
782 transformed uV^2) during resting state (eyes open). Note: Error bars represent SE; $p = .002$ after bootstrapping
783 in cathodal condition.
784
785 **Fig. 6.** Effect of condition (sham, cathodal, and anodal) on delta power (pooled across frontal electrodes, log
786 transformed uV^2) during resting state (eyes open). Note: Error bars represent SE; $p = .003$ after bootstrapping
787 in cathodal condition.

788 **Fig. 7.** Effect of condition (sham, cathodal, and anodal) on rTPJ-lTPJ coherence (post-pre stimulation
789 difference) in delta bandwidth during resting state (eyes open). Note: Error bars represent SE; $p = .012$ after
790 bootstrapping for anodal-cathodal comparison; $p = 041$ after bootstrapping for anodal-sham comparison.

791

Table 1

Demographic characteristics as per group.

Variable	Sham (n = 18)		Cathodal (n = 18)		Anodal (n =17)		ANOVA statistics	
	M	*SD*	*M*	*SD*	*M*	*SD*	*F*	*p*
Age	26.5	6.6	24.4	4.4	24.3	5.4	0.90	.41
Years of education	17	2.6	17.3	2.6	17.4	3.4	0.10	.91
Time of day tested	11:34	2.6	11:52	2.6	11:00	2.4	0.20	.82
EHI	0.88	0.2	0.83	0.2	0.85	0.2	0.24	.79

Note: EHI = Edinburgh Handedness Inventory

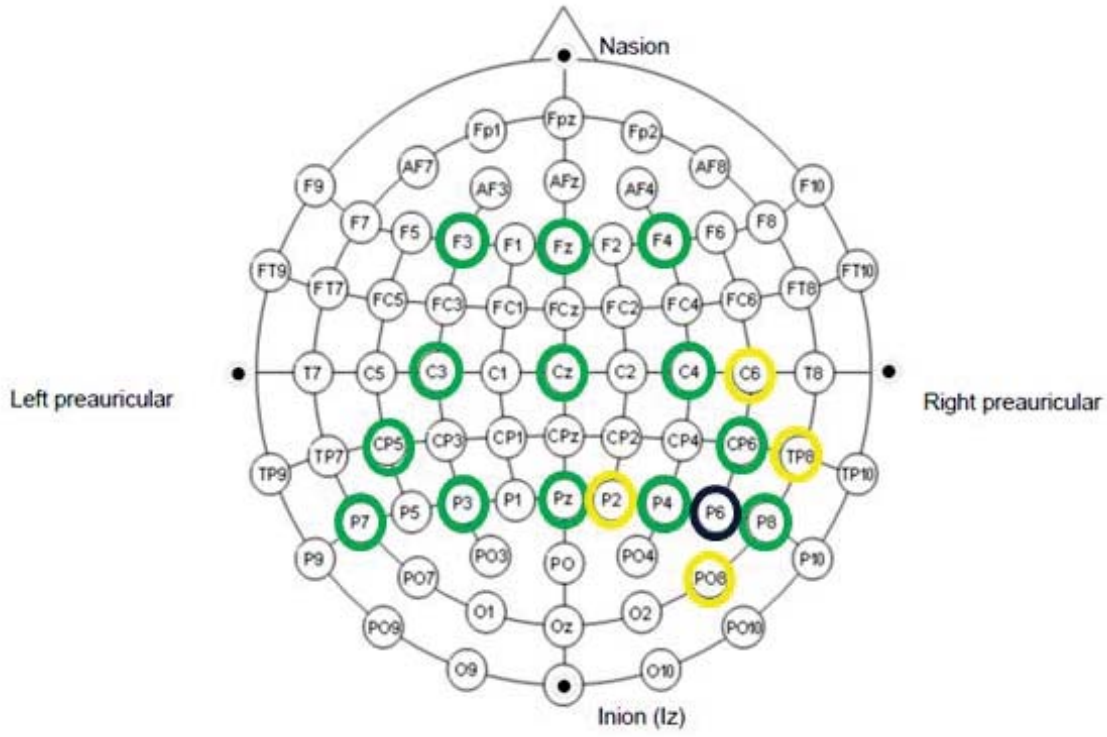

Fig. 1. Diagram of EEG electrode layout (green circles) and HD-tDCS electrode montage (yellow circles 0.5 mA each, navy blue circle 2 mA, polarity depending on anodal or cathodal condition). Electrodes were also placed on each mastoid, above and below the left eye, and on the lateral canthus of each eye. The ground electrode was placed centrally on the forehead.

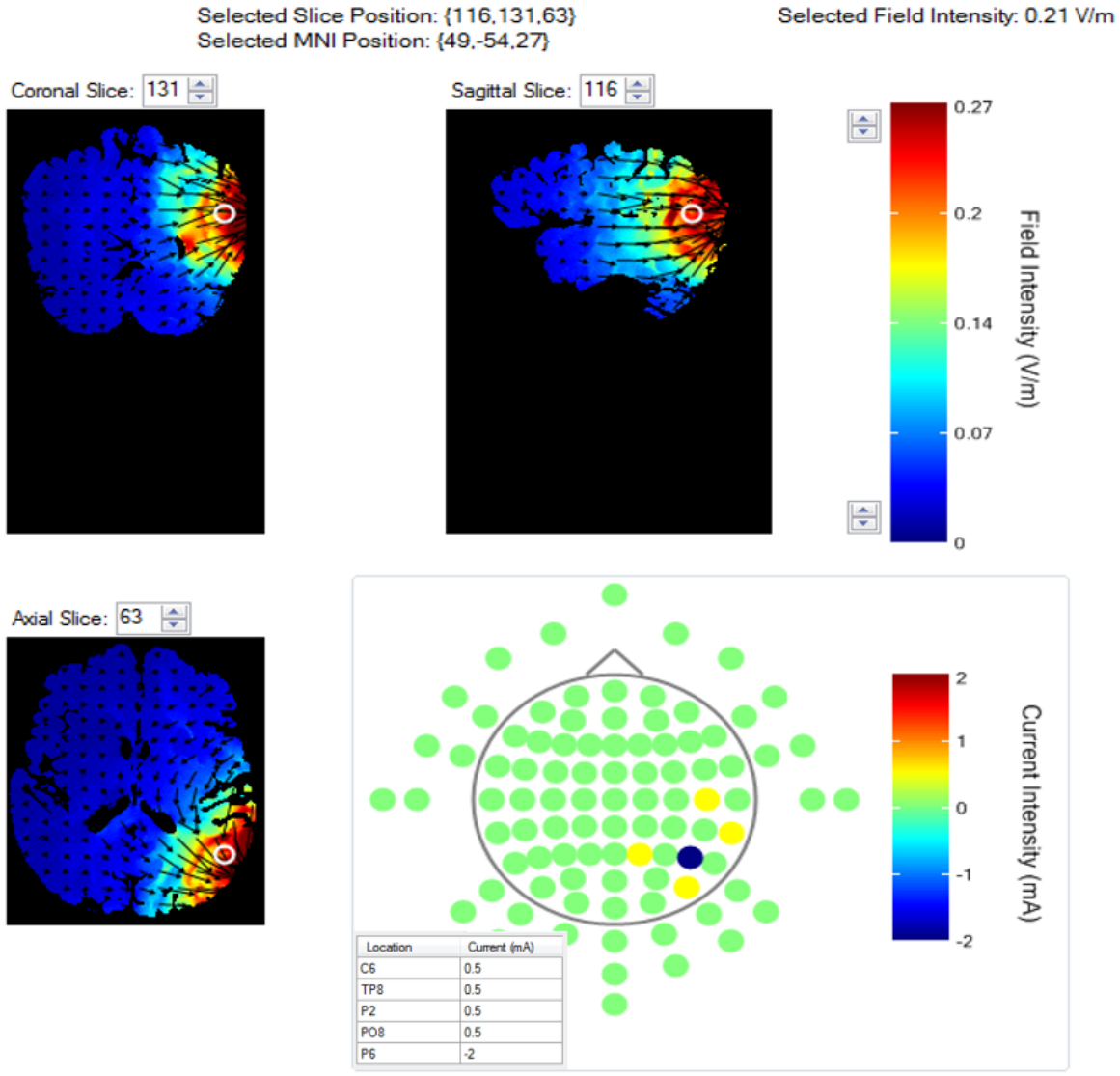

Fig. 2. Montage and Soterix modelling for cathodal stimulation of the rTPJ. Polarities are reversed for anodal stimulation. For anodal stimulation, the central electrode (P6) was the anode, with the other four electrodes (C6, TP8, PO8, P2) collectively forming the cathode (see also Figure 1). The reverse polarity arrangement constituted cathodal stimulation.

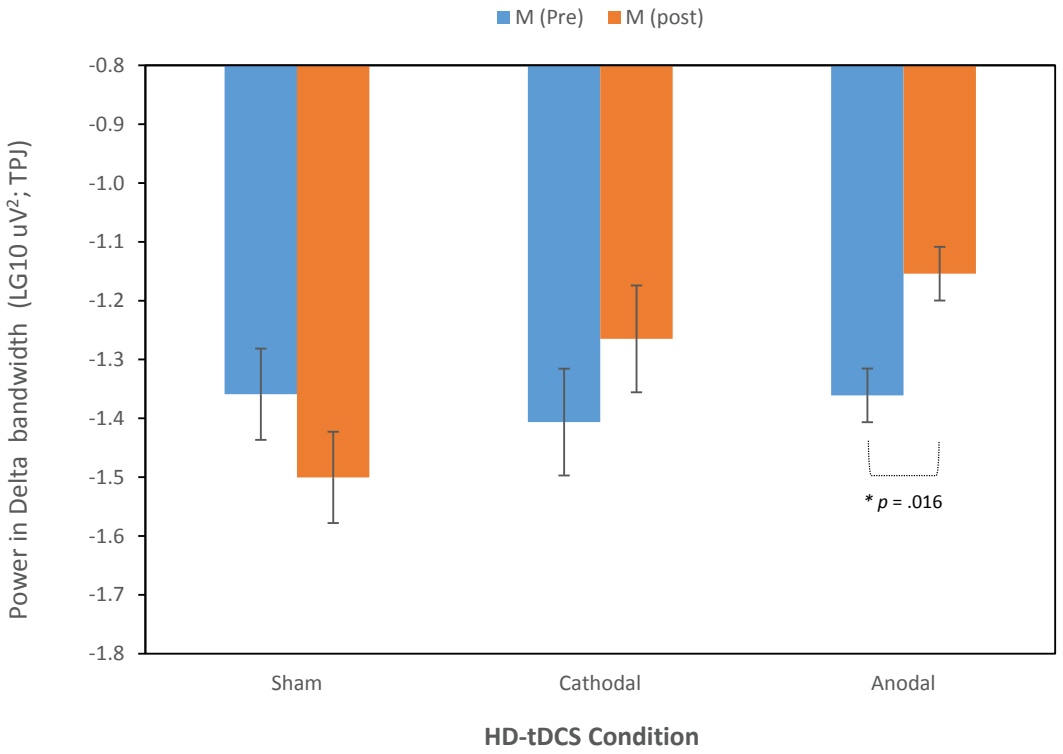

Fig. 3. Effect of condition (sham, cathodal, and anodal) on TPJ delta power (pooled across rTPJ and lTPJ, log transformed uV^2) during resting state (eyes open). Note: Error bars represent SE; $p = .019$ after bootstrapping in anodal condition.

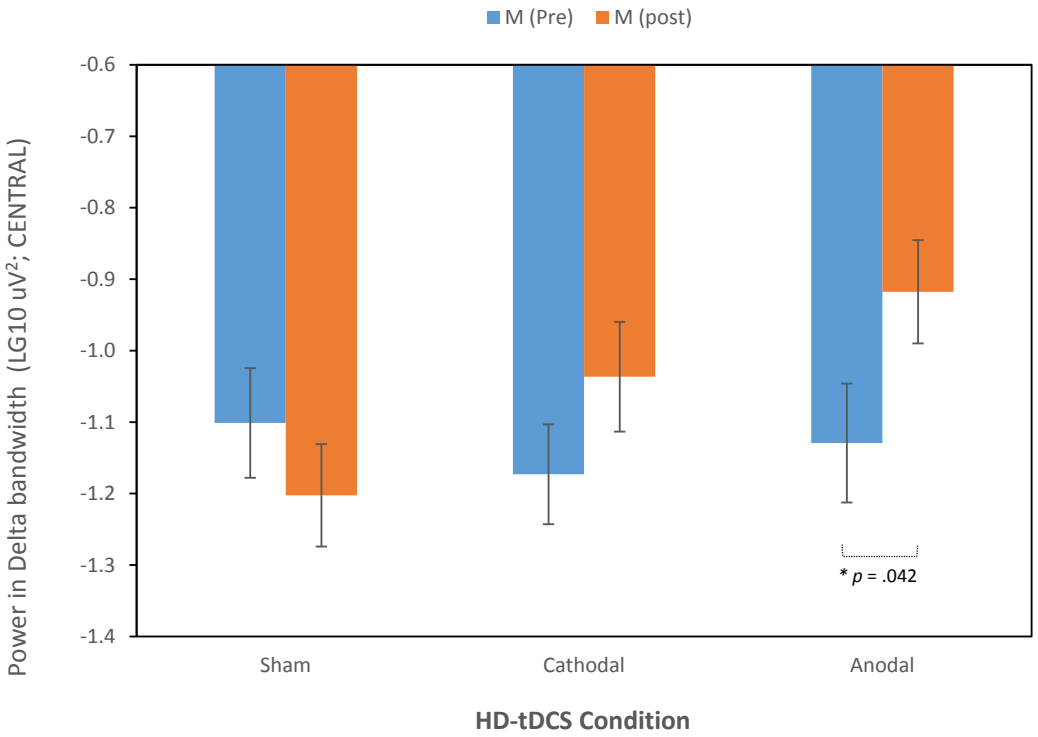

Fig. 4. Effect of condition (sham, cathodal, and anodal) on delta power (pooled across central electrodes, log transformed uV^2) during resting state (eyes open). Note: Error bars represent SE; $p = .052$ after bootstrapping in anodal condition.

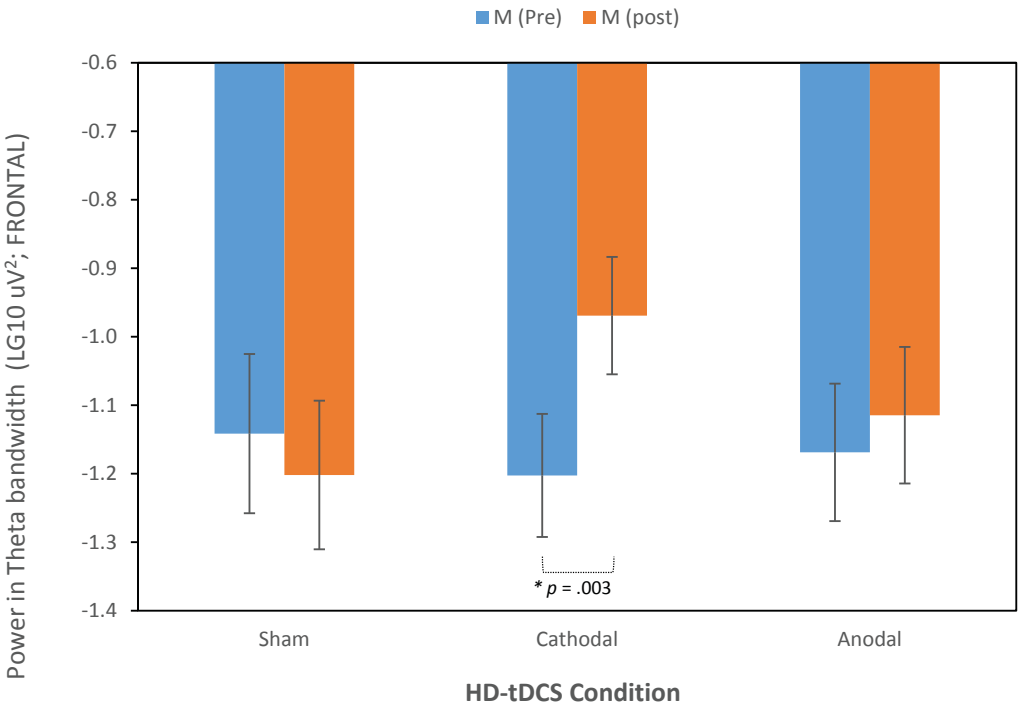

Fig. 5. Effect of condition (sham, cathodal, and anodal) on theta power (pooled across frontal electrodes, log transformed uV^2) during resting state (eyes open). Note: Error bars represent SE; $p = .002$ after bootstrapping in cathodal condition.

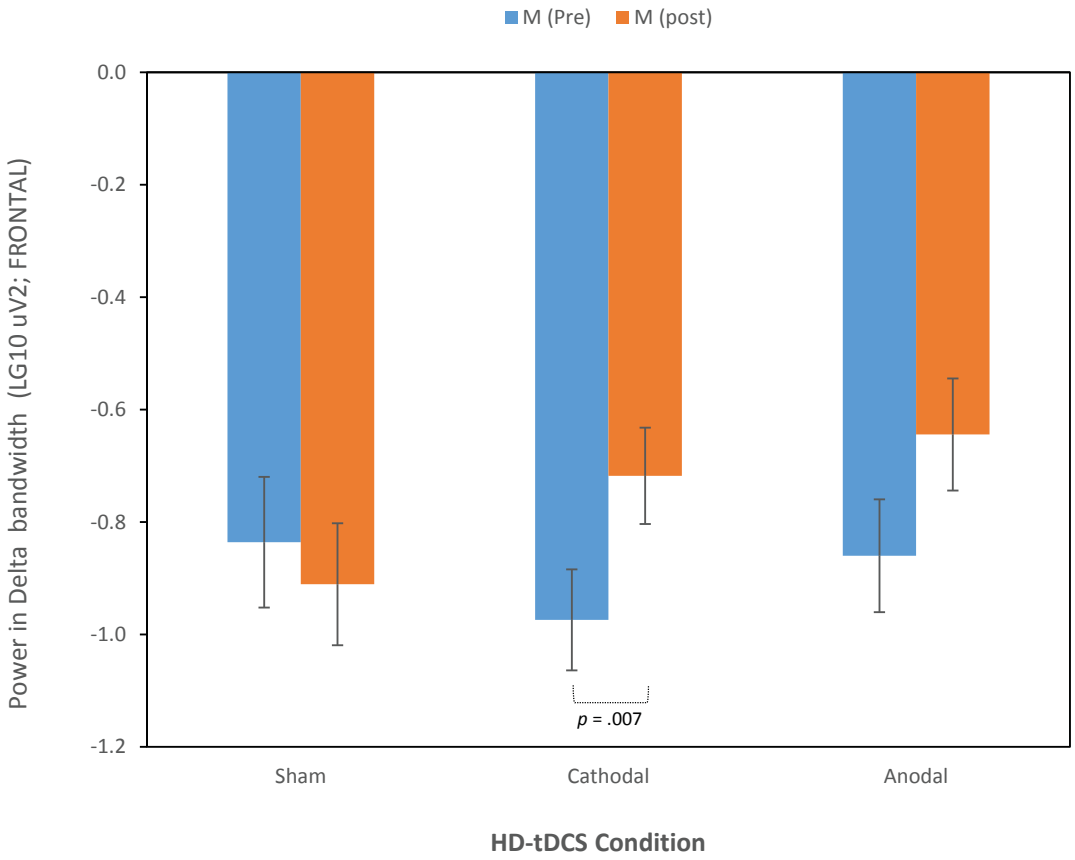

Fig. 6. Effect of condition (sham, cathodal, and anodal) on delta power (pooled across frontal electrodes, log transformed uV^2) during resting state (eyes open). Note: Error bars represent SE; $p = .003$ after bootstrapping in cathodal condition.

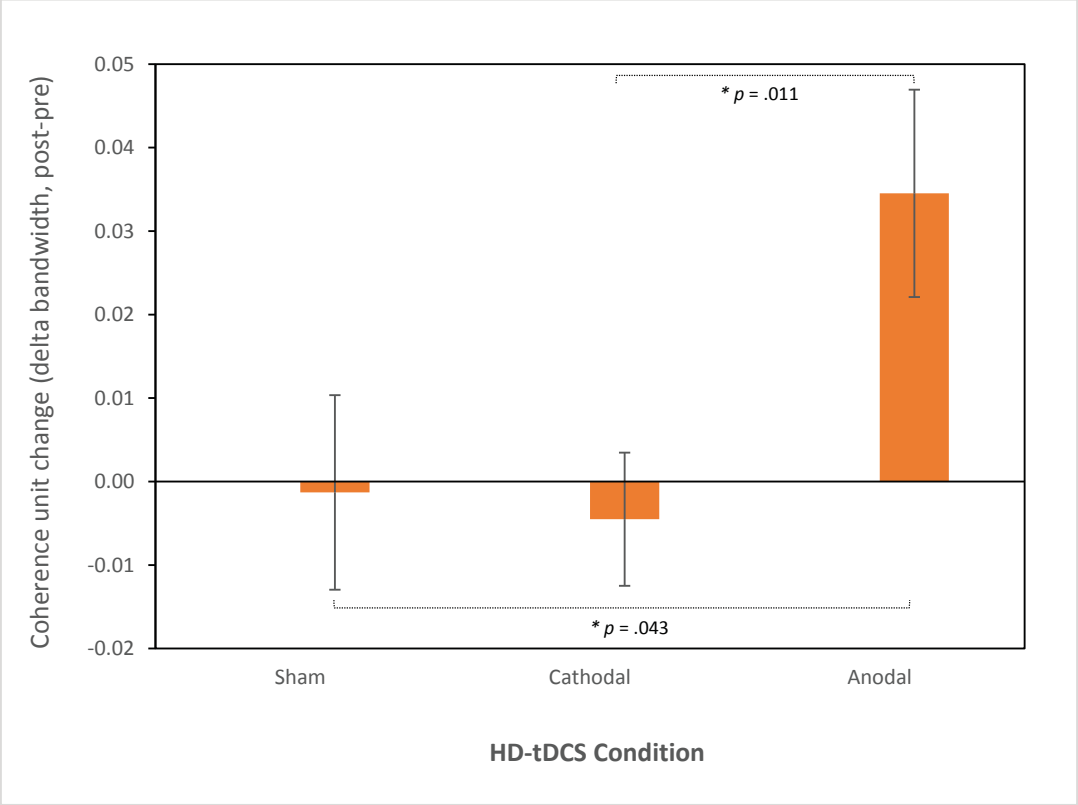

Fig. 7. Effect of condition (sham, cathodal, and anodal) on rTPJ-lTPJ coherence (post-pre stimulation difference) in delta bandwidth during resting state (eyes open). Note: Error bars represent SE; $p = .012$ after bootstrapping for anodal-cathodal comparison; $p = 041$ after bootstrapping for anodal-sham comparison.